MODELING MARTIAN THERMOKARST SUBSIDENCE WITH MAGMATIC MELTING OF PERMAFROST D. McInnis[1], S. E. H. Sakimoto[1], and E. B. Grosfils[2], [1]Department of Civil Engineering and Geological Sciences, 156 Fitzpatrick Hall, University of Notre Dame, Notre Dame, IN, 46556, Email: dmcinnis@nd.edu, ssakimot@nd.edu, [2]Geology Department, Pomona College, Claremont, CA 91711.

Introduction: Volcano- or magma-driven melting of martian ground ice or permafrost (a.k.a. volcano-ice interactions, thermokarst, cryohydrovolcanism, fuel-coolant interactions, etc…) has long been considered a likely and probably even inevetible martian process (e.g., see chapter 5 in [1]) and is an example of types of geothermal-related activity thought to be conducive to forming favorable conditions for potential life. Post-Viking Mars mission data now is available for a wide variety of potential landform evidence consistent with this type of process (e.g. 2-7 and many others). While the melting of ground ice or permafrost by magma chamber emplacement has frequently been suggested by many, unequivocal observational evidence and constraints have proven difficult to obtain. One possible type of landform resulting from magma chamber-permafrost interactions is suggested to be a circum-volcanic topographic moat or depression, where the depression dimensions are dependent on the magma chamber and permafrost extent and properties. Possible examples of this are noted in recent mission data [4,5,7], with an initial simple thermal model assessment [5], and improved magma chamber property constraints [e.g. 8] that allow significantly better thermal model constraints. This study uses additional recent observations and improved modeling capabilities to investigate the time-dependent melting of martian polar region ground ice (permafrost) resulting from the emplacement of a 1 km diameter spherical magma chamber and accompanying lateral sill (the preferred failure mode suggested by [8]) combined with thermal gradient and porosity variations and with as well as without an accompanying surface volcanic edifice. We test the model's predicted melt water volume against observed moat volumes.

Approach: We assume magma chamber and sill configuration to be that of the most-favored failure geometry reported by [8], an then explore the range of accompanying time-dependent thermal solutions described below for transient melting of the permafrost.

General Method: For our model, we assume a basaltic substrate with pore space saturated with ground ice. The background thermal gradients and geometry are assumed (see Table 1), and compared to temperature distributions after magma emplacement. The computed volume of pore space above 273 K thermal contour is assumed to contain liquid water (steam generation is volumetrically minimal), which is allowed to exit the system via unspecified processes. Subsidence follws as pore space empties. This subsidence is assumed to equal the maximum potential topographic thermokarst depression. Thus, the volume of ice melted must be ≥ observed moat volume.

Computational Solution: We use the Heat Transfer portions of the program *COMSOL Multiphysics*, which is capable of multi-component and multi-phase media heat transfer. For boundary and initial conditions, we calculate heat transfer in the rock-ice complex according to the assumed geothermal gradient and observed polar surface temperatures, magma emplacement geometry, radiative surface loss, and probable surface pososity summarized in Table 1. Solutions are then found for Fourier's law to describe heat transfer :

$$\delta_{ts} C_{eq}(\delta T/\delta t) + \nabla(-K_{eq} \nabla T) = Q_H + Q_G + Q_C + Q_R$$

Where temperature (T) is the dependent variable. Heat sources are represented by Q_H (general), Q_G (geothermal), Q_C (convective), and Q_R (radiative). The term δ_{ts} is user-defined coefficient not used here. C_{eq} and K_{eq} are the effective thermal properties of the multi-component media as calculated from the thermal properties and relative proportions of the individual components. C_{eq} and K_{eq} defined as:

$$C_{eq} = \Sigma\theta_{Li}\rho_{Li}C_{p,Li} + \Sigma\theta_{Pi}\rho_{Pi}C_{p,Pi}\Sigma\theta_{Li} + \Sigma\theta_{Pi}$$
$$K_{eq} = \Sigma\theta_{Li}K_{Li} + \Sigma\theta_{Pi}K_{Pi} \;\; \Sigma\theta_{Li} + \Sigma\theta_{Pi}$$

Where θ represents the volume fraction of each component, and component properties are represented by ρ (density), C_p (specific heat capacity), and K (thermal conductivity). The subscripts L and P denote liquid and solid properties, respectively, and In our model, L rep-

Fig. 1. A possible magma chamber-permafrost interaction landform: MOLA topography of a volcanic "moat" [7].

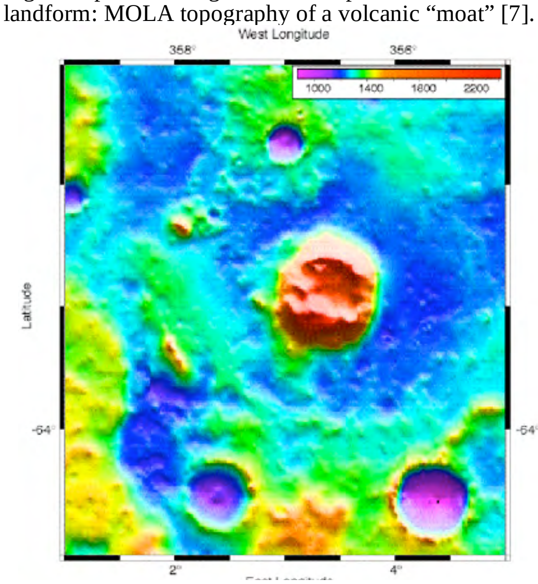

resents pore ice and P represents host rock. Magma is included as a separate initially molten subdomain of uniform composition. Boundary conditions were set to the thermal-gradient-controlled temperature at depth, observed polar surface temperatures and the associated radiative flux at the surface, and symmetry/insulated center and far-field conditions, respectively.. All model parameter values and renges and their source references are summarized in Table 1.

Results and Conclusions: Results are summarized in Figure 2 for those model runs producing melted ice volumes at least as large as the observed moat volumes. In brief, higher than average thermal gradient, surface temperatures, or porsities (or all three) are necessary to produce these features, which likely explains their limited extent and distribution.

References: [1] Carr M.H., (1995) Water on Mars, Oxford Press; [2] Kargel, J.S. et al., (2004) LPSC Abstr. #1995; [3] Ogawa, Y., et al., (2003) JGR, 108, Journal of Geophysical Research (Planets) 108, 2003JGRE.108dGDS27O; [4] Chase, Z.A.J. and S.E.H. Sakimoto, (2003) LPSC Abstr. #1905; [5] Grosfils, E.B. and S.E.H. Sakimoto, S.E.H. (2001) LPSC Abstr., pp1111-1112; [6] Wilson, L. and J.W. Head (2002) In: Smellie, J.L. and M.G. Chapman, M.G. (eds)., GSL Spec. Pub. 202, pp. 5-26; [7] Polit, A. et al., (2003) LPSC Abstr. # 1514; [8] Grosfils, E.B. (2006) LPSC Abstr. # 1015; [9] McGovern, P. J. et al., (2004) JGR, 109 E07007, DOI: 10.1029/2004JE002286; [10] Clifford, S.M. (1981) 3rd International Mars Coll., LPI Contribution 441, 46-48; [11] Annen, C. and R.S.J. Sparks (2002) EPSL, 203(3-4), 937-955; [12] Hobbs, P. V. (1974) Ice Physics. Clarendon Press, Oxford; [13] Burov, E., et al., (2003) JGR, 108(B4), 2177, DOI: 10.1029/2002JB001904; [14] Petford, N. and K. Gallagher, (2001) EPSL, 193(3-4), 483-499; [15] Clifford, S.M. (1981) 3rd International Mars Coll., LPI Contribution 441, 46-48;[16] Clifford, S.M. and F.P. Fanale, (1985) LPSC Abstr., pp.144-145; [17] Clifford, S.M. (1993) LPSC Abstr., pp. 313-314; [18] Ohring, G. and J. Mariano (1968) J Atmos. Sci., 25(5), 673-681; [19]A. Parthare, pers. Comm.. 2006; [20] Slack, G. A. (1980) Phys. Rev. B, 22(6), 3065-3071; [21] Solomon, S.C. and J.W. Head, (1989). LPSCAbstr., pp. 1030-1031; [22] Ruiz, J., et al., (2006) Icarus, 180(2), 308-313; [23] Andersson, O. (1994) Phys. Rev. B, 50(10), 6583-6588; [24] Urquhart, M. L. (2005) LPSC Abstr. #2337.

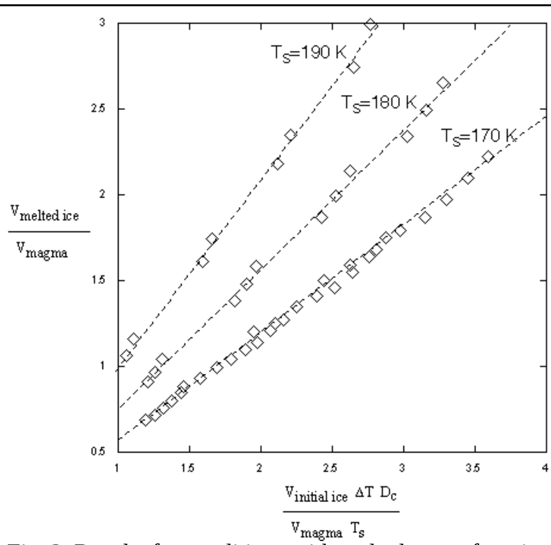

Fig. 2. Results for conditions with melted permafrost ice volumes > observed moat volumes. Plot shows melted ice volume as fraction of initial magma volume vs initial ice volume, thermal gradient, chamber depth, magma intrusion volume and surface temperature. Contoured by best-fit lines for surface temperature. Variations from fits are due to volume summation errors

Acknowledgements: This research was supported in part by a NASA Mars Data Analysis Grant to EBG and SEHS.

Symbol	Parameter	Units	Value(s)	Source(s)
∇T	thermal gradient	K/m	0.005-0.022	[9, 21, 22]
ϕ_s	surface porosity	-	0.2-0.5	[10]
ϕ	porosity	-	ϕ_s*exp(y/2820)	[10,15,17]
ρ_r	density of host rock	kg/m^3	2800	[4,11,5]
ρ_m	density of magma	kg/m^3	2800	[4, 11, 5]
ρ_i	density of ice	kg/m^3	917	[10]
k_i	thermal conductivity of ice	W/m-K	0.468+(488/T)	[12, 20, 23]
k_m	thermal conductivity of magma	W/m-K	2.5	[11,13]
k_r	thermal conductivity of host rock	W/m-K	2.5	[11, 13, 16, 24]
$C_{p,i}$	specific heat of ice	J/kg-K	2000	[10]
$C_{p,m}$	specific heat of magma	J/kg-K	1450	[4,11,5]
$C_{p,r}$	specific heat of host rock	J/kg-K	1450	[4,11,5]
T_s	surface temperature	K	170-190	[18, 19]
T_m	initial temperature of magma	K	1473	[4,14]
V_m	volume of intruded magma	m^3	3.89E+11	[8]-
D_c	depth to magma cham-	m	3000	[8]-